Supplementary Information for

Constraining Amazonian land surface temperature sensitivity to precipitation and the probability of forest dieback

Yuanfang Chai[1], Guilherme Martins[2], Carlos Nobre[2], Celso von Randow[2], Tiexi Chen[3] and Han Dolman[1,3*]

[1] Department of Earth Sciences, Free University Amsterdam, Netherlands.

[2] INPE-CCST, São José dos Campos, Brasil.

[3] School of Geography, Nanjing University of Science and Technology, Nanjing, China.

Corresponding author: Han Dolman

Address: Department of Earth Sciences, Free University Amsterdam, Netherlands.

Tel: +31-20-5987358

Email: han.dolman@vu.nl

ORCIDS: http://orcid.org/0000-0003-0099-0457

This PDF file includes:

- Supplementary Figs. 1 to 11
- Supplementary Tables 1 to 4

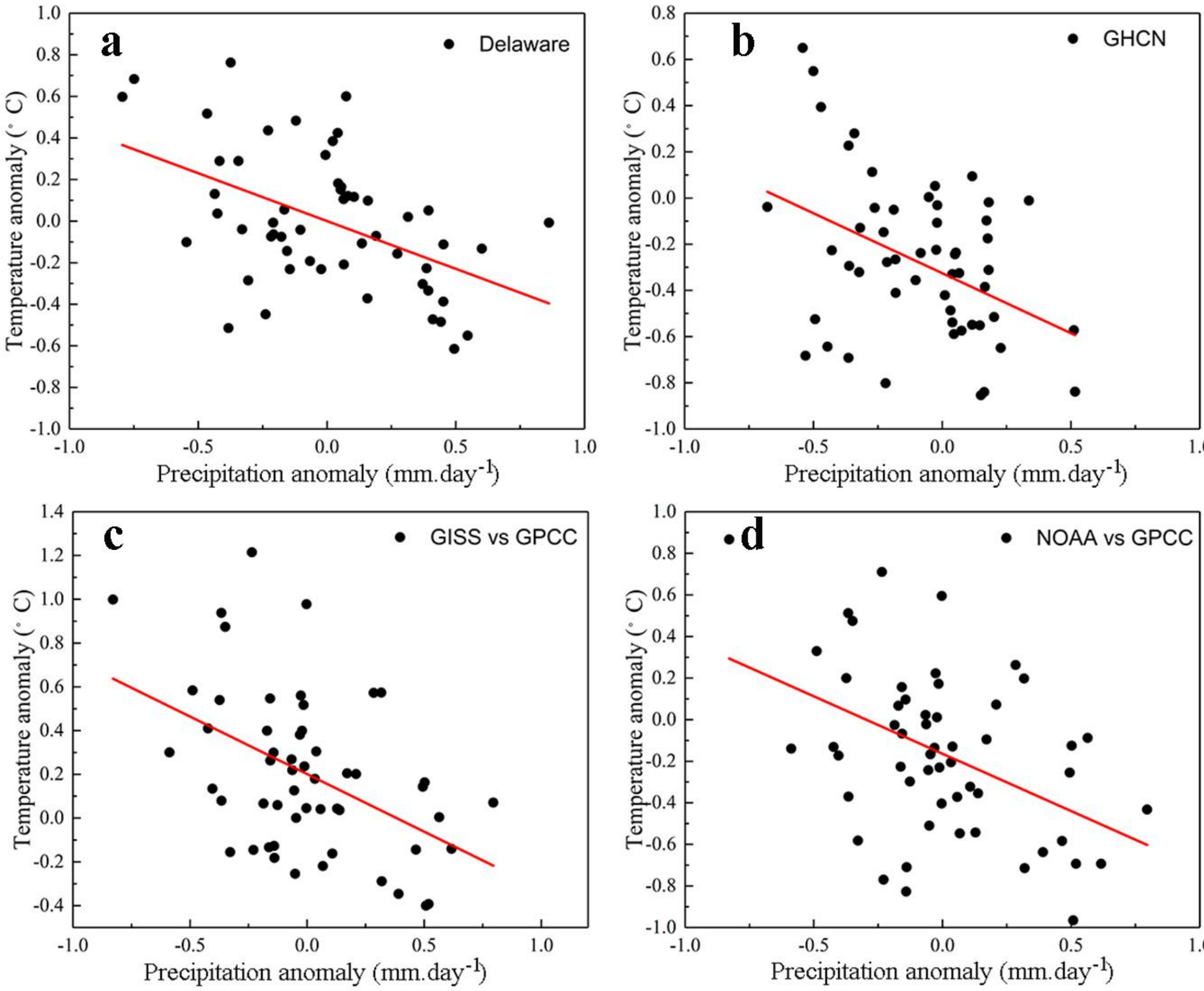

Supplementary Fig. 1: Linear relationships between the observed dry-season temperature anomaly and the observed dry-season precipitation anomaly based on the four data sets of global temperature and precipitation (see the detailed information in Table S1). **(a)**, **(b)**, **(c)** and **(d)** present the linear relationships for the data sets of Delaware (y=(-0.46 ± 0.11)x, p<0.005, R=0.49), GHCN (y=(-0.52 ± 0.16)x-0.33, p<0.005, R=0.4), GISS vs GPCC (y=(-0.53 ± 0.13)x+0.2, p<0.005, R=0.47) and NOAA vs GPCC (y=(-0.55 ± 0.15)x-0.16, p<0.005, R=0.46), respectively.

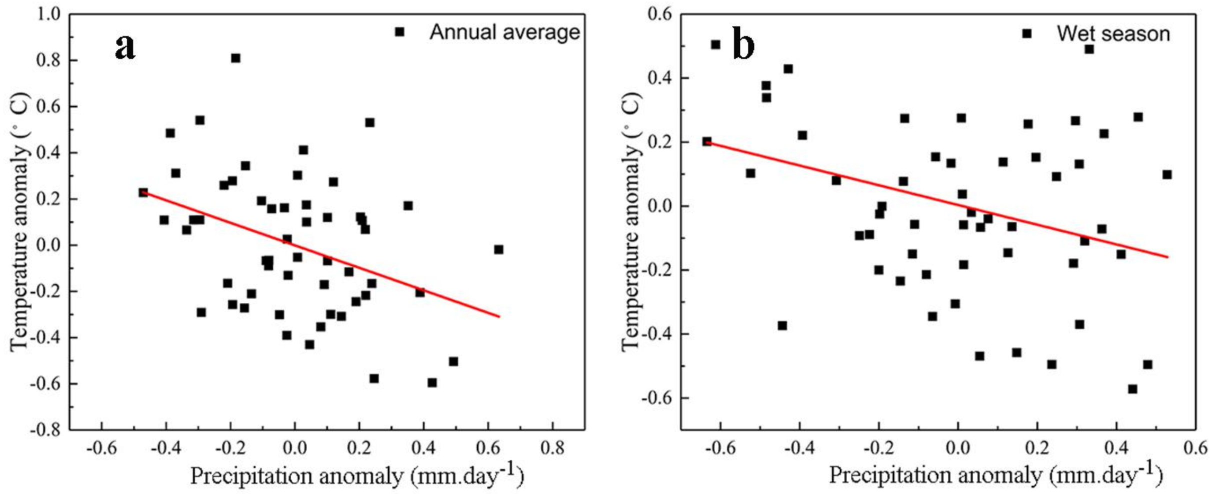

Supplementary Fig. 2: Linear relationship (1949–2002) between the observed temperature anomaly and the observed precipitation anomaly. (a) at the annual scale, y=(-0.49 ± 0.16)x, p<0.001, R=0.39; and **(b)** during the wet season, y=(-0.31 ± 0.13)x, p=0.021, R=0.30, respectively.

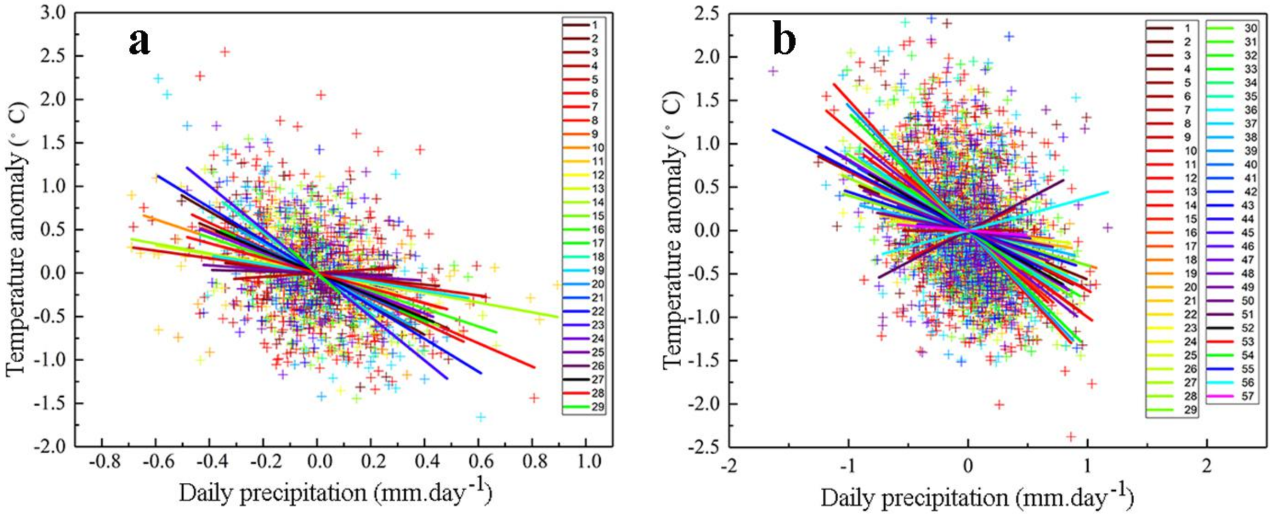

Supplementary Fig. 3: Linear relationships between the simulated historical dry season temperature anomaly and the simulated historical dry season precipitation anomaly. Outputs from **(a)** the 29-member ensemble of CMIP5 models and **(b)** from the 57 model runs comprising the HadCM3 ensemble.

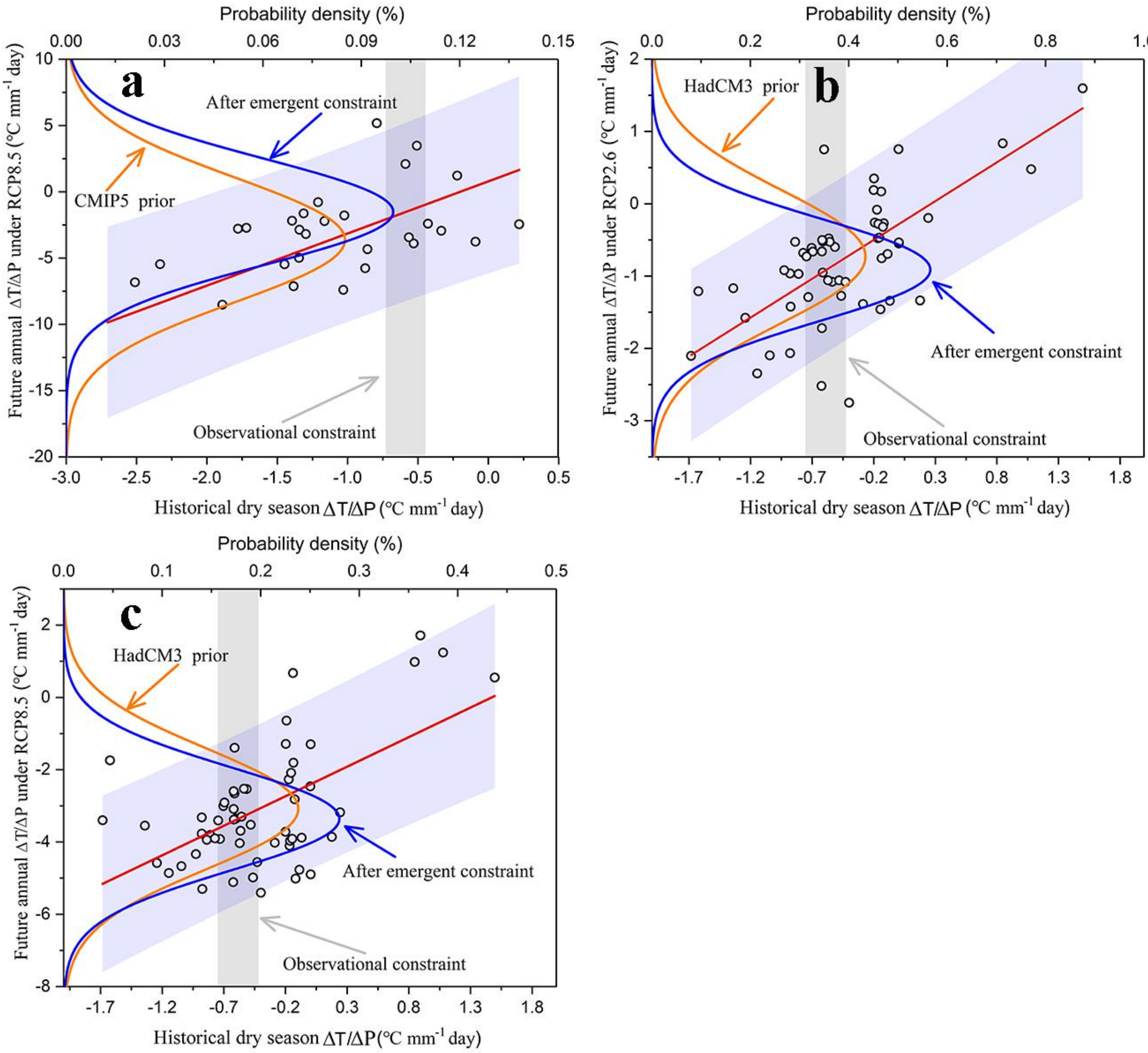

Supplementary Fig. 4: Emergent constraint on the surface air temperature sensitivity to the precipitation. (a) The outputs from the 29-model CMIP5 ensemble under RCP8.5. The linear regression relationship between the future annual temperature sensitivity during 2006–2098 (left y-axis) and the historical dry-season temperature sensitivity during 1949–2002 (bottom x-axis) (y=(3.93 ± 1.0)x+0.79, p<0.001, R=0.60); each model is shown by a single black circle; **(b)** and **(c)** are the linear regression relationships for the 57-model the HadCM3 ensemble under RCP2.6 (y=(1.07 ± 0.15)x-0.29, p<0.001, R=0.68) and under RCP8.5 (y=(1.63 ± 0.32)x-2.41, p<0.001, R=0.57), respectively. The grey shading is the observational constraint from the HadCRUT4 data (Observed value ± 1 standard error, -0.58±0.16 ^{o}C mm^{-1} day). The blue shading represents the 90% prediction error of the linear fitting that has taken the fitting errors into consideration after the application of the emergent constraint. The orange and blue curves represents the probability density functions (PDFs) for the future annual temperature sensitivities before and after the application of the emergent constraint. All models are assumed to obey a Gaussian distribution;

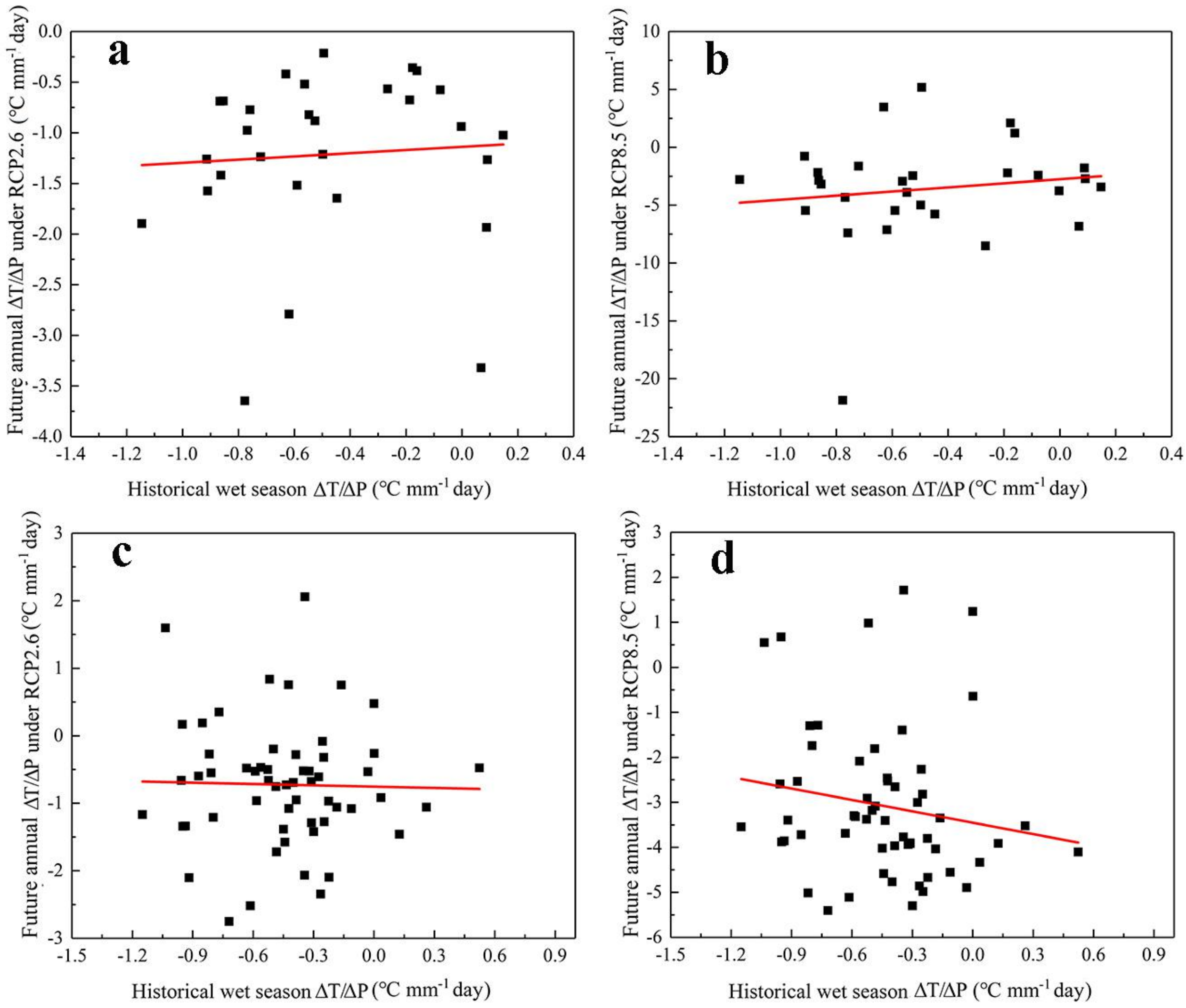

Supplementary Fig. 5: Linear relationships between the future annual temperature sensitivity and the historical wet-season temperature sensitivity. Using the outputs from the 29 models of the CMIP5, **(a)** and **(b)** are the linear regression relationships between the future annual temperature sensitivity during 2006–2098 (left y-axis) and the historical wet season temperature sensitivity during 1949–2002 (bottom x-axis) under RCP2.6 (y=(0.16 ± 0.45)x-1.14, p>0.7, R=0.07) and RCP8.5 (y=(1.77 ± 2.47)x-2.76, p>0.4, R=0.13), respectively; Similarly, using the outputs from the 57 HadCM3 model runs, **(c)** and **(d)** present the linear regression relationships between the future annual temperature sensitivity and historical wet season temperature sensitivity under RCP2.6 (y=(-0.06 ± 0.37)x-0.75, p>0.8, R=0.02) and RCP8.5 (y=(-0.84 ± 0.66)x-0.345, p>0.2, R=0.16), respectively;

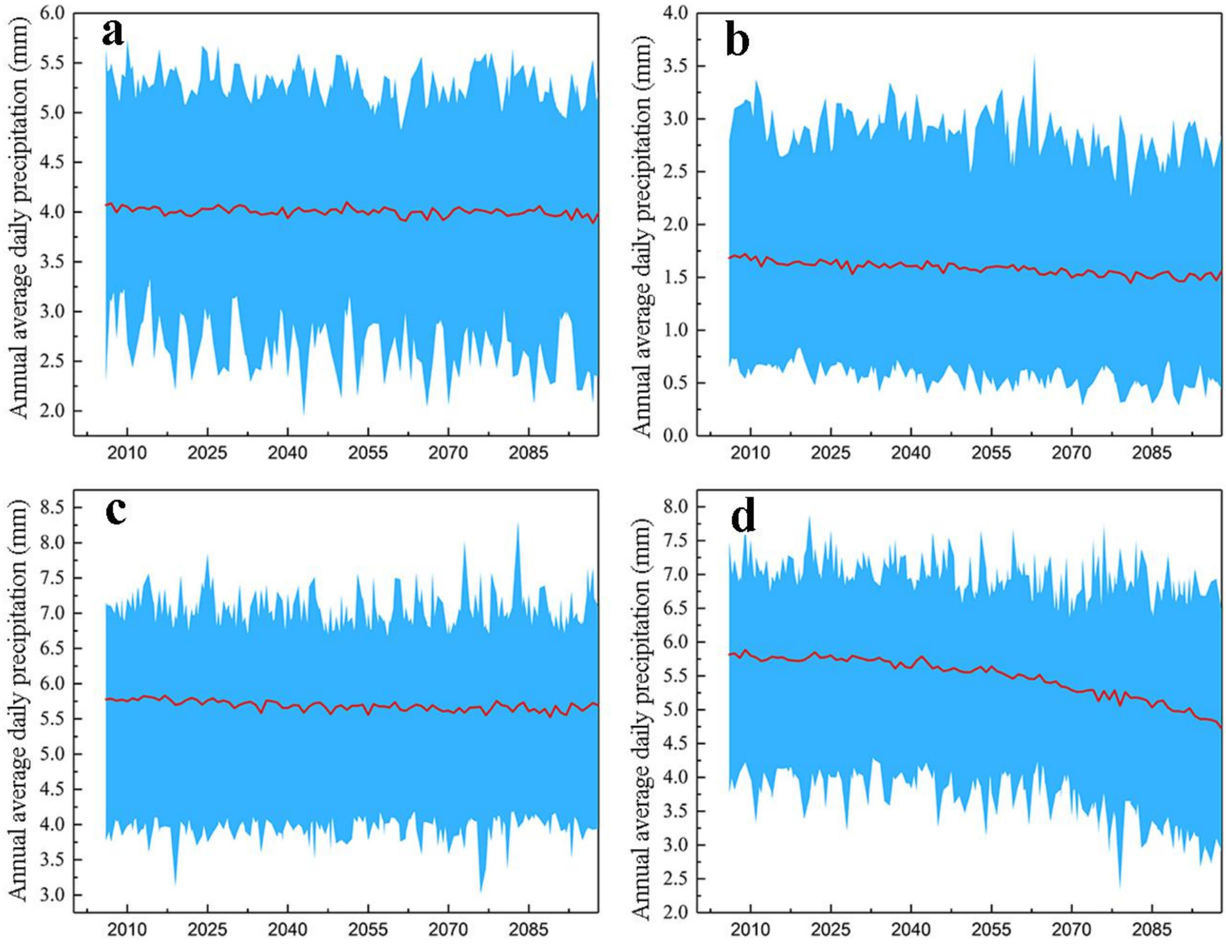

Supplementary Fig. 6: Variation trends in the future annual average daily Amazonian precipitation during 2006–2098. (a) and **(b)** are the trends in future precipitation using the outputs from the 29-model CMIP5 ensemble under RCP2.6 and under RCP8.5, respectively; **(c)** and **(d)** are the trends in future precipitation using the outputs from the 57-member ensemble of HadCM3 model runs under RCP2.6 and under RCP8.5, respectively. The red lines are the mean trends: the differences in multi-year average precipitation between the periods of 2089–2098 and 2006–2015 are -0.08 mm day^{-1} (CMIP5 under RCP2.6), -0.17 mm day^{-1} (CMIP5 under RCP8.5), -0.14 mm day^{-1} (HadCM3 under RCP2.6) and -0.80 mm day^{-1} (HadCM3 under RCP8.5).

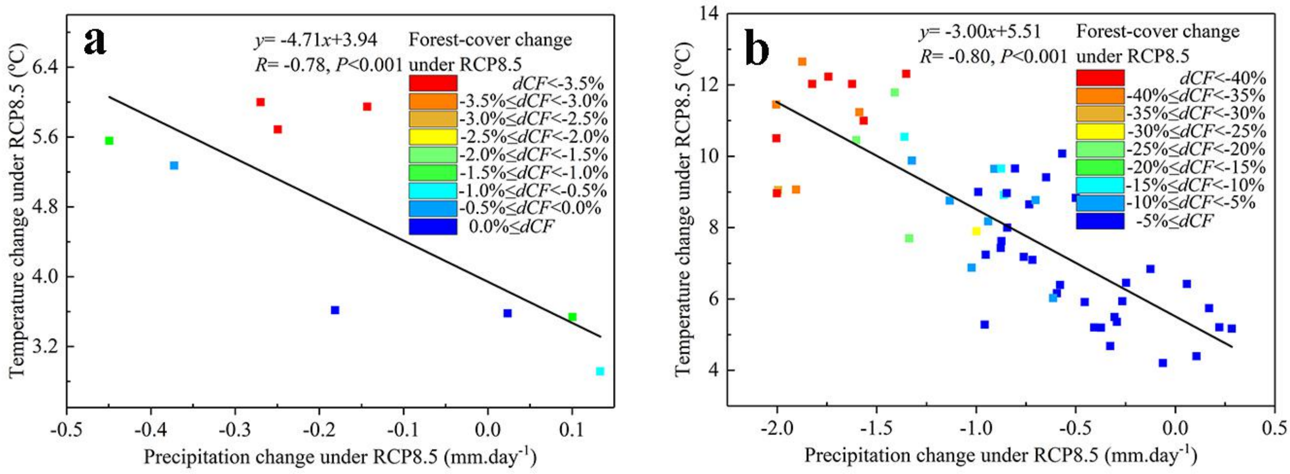

Supplementary Fig. 7: Linear relation between the future changes in precipitation and temperature for the CMIP5 models (a) and the HadCM3 models (b) under RCP8.5 during the period of 2089–2098 in relative to the period of 2006–2015.

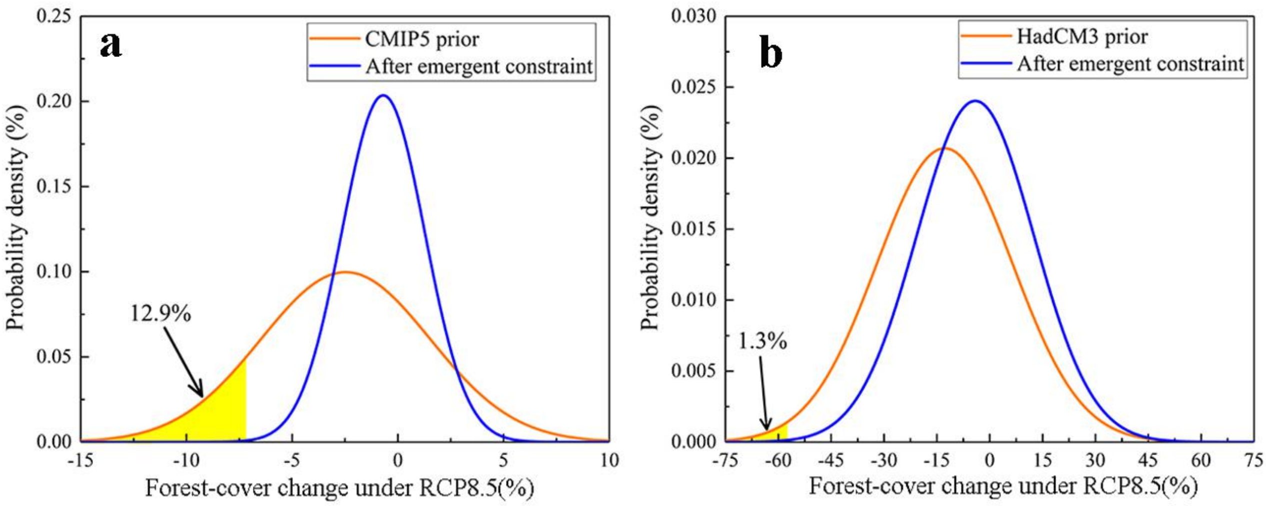

Supplementary Fig. 8: PDF for the future forest losses in response to the mean temperature sensitivity from the original outputs of the CMIP5 models (prior outputs) and in response to the constrained temperature sensitivity ("emergent constraint"). Based on the PDF for the initial vegetation cover, the probability of the forest losses being higher than 7% is 12.9% for the CMIP5 models under RCP8.5. Under the constrained precipitation sensitivity, this will not occur. For the HadCM3 models under RCP 8.5, the probability of the initial forest losses higher than 57% is 1.3%. Under the constrained temperature sensitivity, this will also not occur.

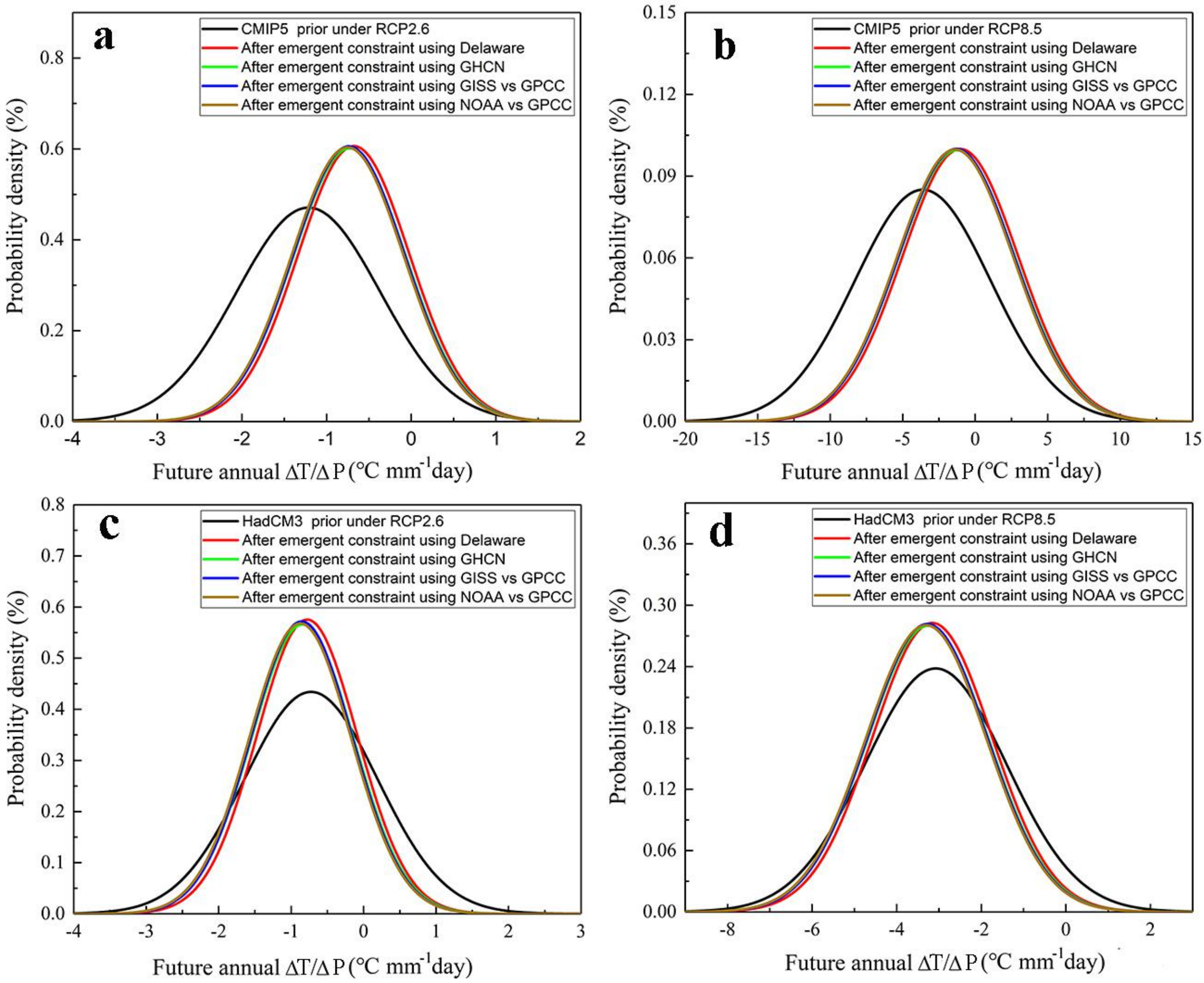

Supplementary Fig. 9: PDF for the future temperature sensitivity to the precipitation change before and after the observational constraint by using the four data sets. (a) and **(b)** are PDF for the CMIP5 models under RCP2.6 and under RCP8.5, respectively. **(c)** and **(d)** are the PDF for the HadCM3 model runs under RCP2.6 and under RCP8.5, respectively.

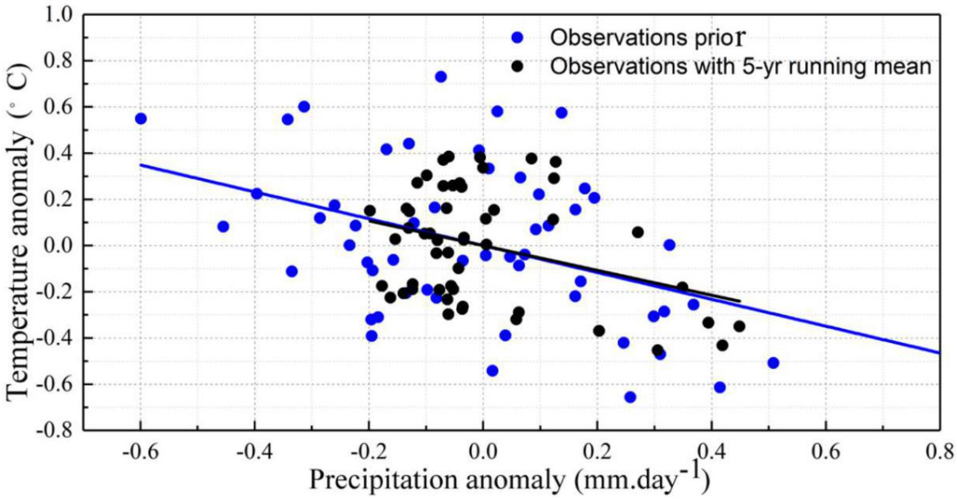

Supplementary Fig. 10: Linear relationships between the seasonal average temperature anomaly and the seasonal average precipitation anomaly during 1949–2002. Blue line and black lines are the linear relationships for the initial observations (y=(-0.58 ± 0.16)x, p<0.001, R=0.45) and for the observations with 5-year running mean (y=(-0.54 ± 0.08)x, p<0.01, R=0.34), respectively. Note: during 1949–2002, 12 El Niño events occurred with the frequency of around 5 El Niño events a year. Thus, the 5-year running mean is used here to smooth out the extreme fluctuations caused by El Niño events and highlight longer-term trends.

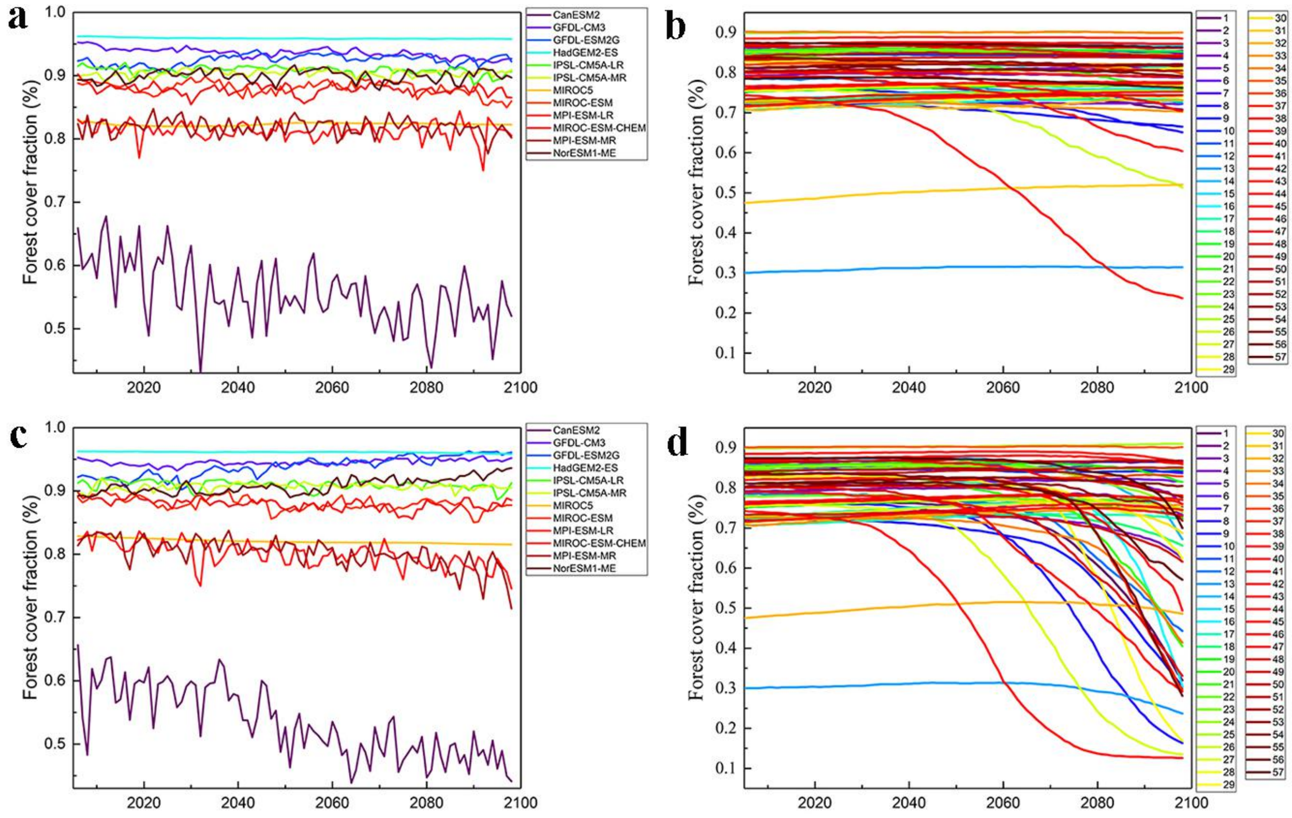

Supplementary Fig. 11: Changes in the Amazonian forest-cover fraction during 2006–2098. (a) and **(c)** are the changes for the CMIP5 models under RCP2.6 and RCP8.5, respectively; **(b)** and **(d)** are the changes for the HadCM3 model runs under RCP2.6 and RCP8.5, respectively;

Supplementary Table 1. Observed global precipitation and temperature data sets.

Name	Source	Spatial Resolution	Spatial Coverage	Temporal Resolution
HadCRUT4	The CRU of the University of East Anglia	0.5°×0.5°	90N - 90S, 0E - 360E	Monthly
Delaware V5.01	University of Delaware	0.5°×0.5°	89.75N-89.75S, 0.25E-359.75E	Monthly
GHCN	National Climatic Data Center; Arizona State University; Carbon Dioxide Information Analysis Center;	5°×5°	87.5S-87.5N, 2.5E - 357.5E	Monthly
NOAA	National Oceanic and Atmospheric Administration	5°×5°	87.5S-87.5N, 2.5E - 357.5E	Monthly
GISS	Goddard Institute for Space Studies	2°×2°	89.0N - 80.0S, 1.0E - 359.5E	Monthly
GPCC	Global precipitation climatology centre	0.5°×0.5°	89.75N-89.75S, 0.25E-359.75E	Monthly

Supplementary Table 2. Full name of the 29 CMIP5 models. Note: Only one ensemble member from each model was selected; The model 29 represents the ensemble mean of the CMIP5 models.

Number in Fig. S3	Model name	Number in Fig. S3	Model name
1	BCC-CSM1-1-M	16	GISS-E2-R
2	BCC-CSM1-1	17	GFDL-CM3
3	NorESM1-ME	18	GFDL-ESM2G
4	NorESM1-M	19	FIO-ESM
5	MRI-CGCM3	20	EC-EARTH
6	MPI-ESM-LR	21	FGOALS-g2
7	MPI-ESM-MR	22	CanESM2
8	MIROC5	23	CSIRO-Mk3-6-0
9	MIROC-ESM-CHEM	24	CNRM-CM5
10	MIROC-ESM	25	CESM1-WACCM
11	IPSL-CM5A-LR	26	CESM1-CAM5
12	IPSL-CM5A-MR	27	CCSM4
13	HadGEM2-AO	28	BNU-ESM
14	HadGEM2-ES	29	Ensemble
15	GISS-E2-H		

Supplementary Table 3. Emergent constraint on precipitation sensitivity ($\Delta T/\Delta P$, °C mm^{-1} day) using the HadCRUT4 data set under 66% confidence limits.

		Before emergent constraint		After emergent constraint	
		Mean value	Range under 66% confidence limits	Mean value	Range under 66% confidence limits
CMIP5 models	RCP2.6	-1.22	±0.79	-0.78	±0.63
	RCP8.5	-3.62	±4.46	-1.49	±3.83
HadCM3 models	RCP2.6	-0.73	±0.87	-0.91	±0.67
	RCP8.5	-3.08	±1.59	-3.35	±1.35

Supplementary Table 4. Emergent constraint on temperature sensitivity (Δ*T*/Δ*P*, °C mm^{-1} day**) based on the four other data sets.** Note: The identified "tipping point" in this study is the precipitation sensitivity at -3.41 °C mm^{-1} day. The central estimates of the constrained temperature sensitivities under RCP8.5 in the table below did not all cross the tipping point, neither for the CMIP5 models nor for the HadCM3 models. This result is in agreement with the conclusions of the emergent constraint with the HadCRUT4.

	Observed seasonal sensitivity ± one standard deviation			After emergent constraint		Underestimated temperature increase (°C)
				Mean value	Range under 66% confidence limits	
Delaware	-0.46 ± 0.11	CMIP5 models	RCP2.6	-0.68	0.63	-0.043
			RCP8.5	-1.02	3.8	-0.442
		HadCM3 models	RCP2.6	-0.78	0.66	0.007
			RCP8.5	-3.16	1.35	0.064
GHCN	-0.52 ± 0.16	CMIP5 models	RCP2.6	-0.73	0.64	-0.039
			RCP8.5	-1.26	3.91	-0.401
		HadCM3 models	RCP2.6	-0.84	0.66	0.015
			RCP8.5	-3.26	1.36	0.144
GISS vs GPCC	-0.53 ± 0.13	CMIP5 models	RCP2.6	-0.73	0.64	-0.039
			RCP8.5	-1.30	3.92	-0.394
		HadCM3 models	RCP2.6	-0.85	0.65	0.017
			RCP8.5	-3.27	1.34	0.152
NOAA vs GPCC	-0.55 ± 0.15	CMIP5 models	RCP2.6	-0.75	0.63	-0.038
			RCP8.5	-1.38	3.92	-0.381
		HadCM3 models	RCP2.6	-0.88	0.66	0.021
			RCP8.5	-3.31	-1.35	0.184